PCCP

A quasiclassical trajectory and quantum mechanical study of the $O(^1D) + D_2$ reaction dynamics. Comparison with high resolution molecular beam experiments

F. J. Aoiz,[a] L. Bañares,[a] J. F. Castillo,[a] V. J. Herrero[b] and B. Martínez-Haya[c]

[a] *Departamento de Química Física, Facultad de Química, Universidad Complutense, 28040, Madrid, Spain*
[b] *Instituto de Estructura de la Materia (CSIC), Serrano 123, 28006 , Madrid, Spain*
[c] *Departamento de Ciencias Ambientales, Universidad Pablo de Olavide, E-41013 , Seville, Spain*

Received 17th April 2002, Accepted 27th June 2002
First published as an Advance Article on the web 2nd August 2002

A theoretical study of the dynamics of the $O(^1D) + D_2$ reaction has been performed at the collision energies (E_c = 86.7 meV and 138.8 meV) of a recent high resolution molecular beam experiment using the D-atom Rydberg "tagging" technique (X. Liu *et al.*, *Phys. Rev. Lett.*, 2001, **86**, 408). The theoretical calculations have been carried out on the *ab initio* $1^1A'$, $1^1A''$ and $2^1A'$ potential energy surfaces (PES) by Dobbyn and Knowles. The quasiclassical trajectory (QCT) method was used for the investigation on the ground electronic PES ($1^1A'$). Non-adiabatic transitions between this PES and the excited $2^1A'$ were considered by using a trajectory surface hopping methodology. An accurate quantum mechanical (QM) approach was used for the reaction on the excited $1^1A'$ PES. The theoretical results are globally in good agreement with the measurements and indicate that, although the excited $1^1A''$ surface does contribute to the reaction at the higher collision energy, a large part of the observed increase in backward reactive scattering is due to the reaction over the ground state $1^1A'$ PES.

I. Introduction

The reaction dynamics of $O(^1D)$ atoms with H_2 is currently a subject of much experimental and theoretical interest.[1,2] Although, in principle, five different potential energy surfaces (PES) correlate with the five-fold degenerate electronic state of the oxygen atom, the reaction is known to be largely controlled by the lowest adiabatic surface ($1^1A'$), at least in the collision energy range investigated thus far. This PES is essentially barrierless and has a deep attractive well corresponding to the ground state of water.[3] In addition to the $1^1A'$ surface, the two first excited PESs ($1^1A''$ and $2^1A'$) can also participate in the reaction, and the conditions and extent of this possible participation are nowadays a much debated issue.

The most recent theoretical calculations of the electronic potential energy surfaces[4–6] indicate that the lowest barrier height on the $1^1A''$ and $2^1A'$ PESs is about 0.10 eV and no significant contributions from excited channels to the reaction should be expected for collision energies below this value. At higher collision energies, the different reaction mechanisms associated with the ground and excited potential surfaces could allow, in principle, the experimental discrimination of their respective reactive yields in spite of the small contribution of the excited-state channels to the global reactivity. Dynamical calculations indicate that the reaction over the ground state PES takes place *via* an insertion mechanism that leads to products isotropically scattered and distributed in a near statistical way over the available internal energy levels. However, reaction over the excited $1^1A''$ PES proceeds *via* an abstraction mechanism, yielding mostly backward scattering (with respect to the incoming atom) and with vibrationally hot and rotationally cold product state distributions. The reaction over the $2^1A'$ surface, which does not correlate with ground state products, can take place by means of non-adiabatic coupling through a conical intersection with the ground $1^1A'$ state. The products from this channel would exhibit a mixture of the characteristics of the insertion and abstraction mechanisms.

In an attempt to identify the distinctive features commented on above, various research groups have performed experiments on this reactive system using different experimental methods (see refs. 7–20 and references therein). The highest resolution measurements reported thus far have been carried out by Yang and co-workers[17–20] using the Rydberg atom "tagging" technique. In these experiments rovibrational state resolution in the products was achieved for selected scattering angles. The method was first applied to the study of the $O(^1D) + HD$ at E_c = 73.7 meV (1.7 kcal mol^{-1})[17] and of $O(^1D) + H_2$ at E_c = 56.4 meV (1.3 kcal mol^{-1});[18] both collision energies are lower than that of the barrier for reaction on the $1^1A''$ PES. A first analysis of the $O(^1D) + H_2$ experiment suggested that some contribution of the excited $1^1A''$ PES could be identified in the experimental data even at this low collision energy, but a detailed simulation of the measurements with the results of thorough quantum mechanical (QM) and quasiclassical trajectory (QCT) calculations on the $1^1A'$ and $1^1A''$ surfaces[20] has proven the contrary.

In a subsequent work, Liu *et al.*[19] investigated the $O(^1D) + D_2$ reaction at two collision energies, E_c = 86.7 and 138.8 meV (2 and 3.2 kcal mol^{-1}, respectively), one of them again below the classical barrier of the $1^1A''$ PES and the other one above it. An inspection of the experimental data showed that for the higher collision energy the products angular distribution becomes asymmetric with an increase in the amount of backward scattering and that this increase in backward scattering is associated with vibrationally hot and rotationally cold OD molecules. No detailed theoretical investigation has been reported thus far for the conditions of this experiment.

In this article, we present the results of extensive theoretical calculations of the reaction dynamics of $O(^1D) + D_2$ at the two collision energies of the experiment of Liu *et al.*[19] The present study has been carried out on the Dobbyn and Knowles (DK) $1^1A'$, $1^1A''$ and $2^1A'$ PESs.[6] Accurate QM scattering calculations have been performed on the excited $1^1A''$ PES, whereas QCT calculations were carried out on the ground state $1^1A'$ surface. Non-adiabatic contribution from the excited $2^1A'$ PES has been considered by means of a trajectory surface hopping method. In order to compare the theoretical predictions with the measurements, the experimentally determined recoil energy distributions of the products have been simulated with the results of the calculations.

II. Theoretical methods

A. Quasi-classical trajectory method

The quasiclassical trajectory method employed in this work has been described elsewhere (see, for instance, refs. 21–23 and references therein), and only the details relevant to the present work will be given here. Adiabatic and non-adiabatic (surface hopping) QCT calculations have been performed on the DK $1^1A'$ and $2^1A'$ surfaces.

Batches of 200 000 trajectories each were run adiabatically on the $1^1A'$ DK PES at collision energies $E_c = 86.7$ meV (2 kcal mol^{-1}) and $E_c = 138.8$ meV (3.2 kcal mol^{-1}). In both batches, the initial rotational quantum number of D_2, j, was randomly sampled according to a distribution with 67% of $j = 0$ and 33% of $j = 1$ corresponding to the experimental conditions of ref. 19. Trajectories were started at a $O(^1D)$–D_2 distance of 8 Å and a time step of 0.02 fs was employed. Under these conditions total energy was conserved to better than 1 in 10^5. The maximum impact parameters employed were 3.0 Å ($E_c = 86.7$ meV) and 2.65 Å ($E_c = 138.8$ meV).

To consider the non-adiabatic dynamics on the coupled $1^1A'$ and $2^1A'$ PESs at the higher collision energy ($E_c = 138.8$ meV), we have employed the trajectory surface hopping (TSH) method described in ref. 22. Batches of 200 000 trajectories each were run starting on the $1^1A'$ or on the $2^1A'$ DK PESs, respectively, at $E_c = 138.8$ meV using the distribution for the initial rotational quantum number j of D_2 indicated above. The calculations on the $1^1A'$ surface were performed using the same initial conditions as in the adiabatic calculations. For the calculations on the $2^1A'$ surface, a maximum impact parameter of 1.7 Å, was used. At each time step, every trajectory was checked to see whether a point of intersection between the $1^1A'$ and $2^1A'$ surfaces in the diabatic representation had been reached. If so, the Landau–Zener formula was used to compute the probability of transition, P_{12}, from one adiabatic surface to the other. As in our previous work,[22] the TSH methodology adopted here does not allow for hops at atom–diatom separations larger than 1.9 Å and, hence, in the asymptotic region where the two surfaces are degenerated. By allowing hops in the asymptotic region, as it was done for instance in ref. 24, the reactivity assigned to the $2^1A'$ PES is borrowed from that on the $1^1A'$ PES at collision energies below the $2^1A'$ barrier. Therefore, by using the TSH method of ref. 24, the predicted reactivity on the $2^1A'$ PES would be larger at the expense of that on the $1^1A'$ PES. Moreover, the dynamics on the $2^1A'$ PES caused by transitions in the asymptotic region will be that of the $1^1A'$ PES and, thus, the net difference between the dynamics on the $1^1A'$ and the coupled $1^1A'/2^1A'$ will take place at energies above the $2^1A'$ barrier to access the region of the conical intersection. Rigorously speaking, the contribution from each surface alone cannot be separated and what is really meaningful is the coupled dynamics on the $1^1A'/2^1A'$ surfaces. However, in the following we will present results of integral and differential cross sections obtained by using the present TSH method with trajectories starting on the $2^1A'$ surface to show the dynamics arising from non-adiabatic transitions in the region of the conical intersection. Integral and differential cross sections corresponding to the present TSH calculations starting on the ground $1^1A'$ PES are almost indistinguishable from those obtained in the adiabatic QCT calculations performed on the $1^1A'$ PES, and, therefore, they will not be considered further.

The rovibrational energies of the D_2 and OD molecules were calculated by semiclassical quantization of the classical action, using in each case the asymptotic diatomic potential of the PES.[21] The assignment of final product quantum numbers was carried out by equating the square of the rotational angular momentum of the outgoing diatom to $j'(j'+1)\hbar^2$. With the real values so obtained, the vibrational quantum number v' was found by equating the internal energy of the diatom to the corresponding Dunham expansion. The derived values of v' and j' were then rounded to the nearest integer.

Differential cross sections (DCS) were calculated for every rovibrational state of the OD products by the method of moments expansion in Legendre polynomials.[21] The Smirnov–Kolmogorov test was used to decide when to truncate the series. Significance levels higher than 99% could be achieved using 4–12 moments, ensuring good convergence, such that the inclusion of more terms did not produce any significant change.

Since the calculations have been carried out without consideration of spin-orbit and Λ-doublet effects, the OD product is treated as a closed shell molecule. Although there is no general and unambiguous procedure to make the correspondence between the j' and N' quantum numbers, a comparison of the experimental energies of the OD rotational levels for the F_1 and A′ states ($^2\Pi_{3/2}$) with the energy of the OD(v',j') levels calculated using the Dunham expansion obtained with the OD diatomic potential of the PES indicates that the correspondence rule $N' = j'$ represents a good approximation. This procedure is alternative to the usual correspondence rule $N' = j' + 1$. Actually, on the basis of comparison of rotational energies, the $N' = j' + 1$ rule is only valid for the first levels and rapidly deviates to the $N' = j'$ rule as N' increases. Therefore, in order to obtain N' quantum numbers we have equated $N' = j'$. Notice that the use of the correspondence rule $N' = j'$ effectively implies to neglect the cross section of the $v', j' = 0$, states, which, in any case, represents an almost negligible contribution to the total cross section.

B. Quantum mechanical method

QM scattering calculations have been carried out for the $O(^1D) + D_2(v = 0, j = 0,1)$ reactions at $E_{col} = 86.7$ meV and 138.8 meV on the first excited $1^1A''$ DK PES. The calculations were performed following the hyperspherical coordinate scheme described in detail elsewhere.[25] Convergence of the reactive cross sections requires helicity quantum numbers up to $k = 3$. The coupled-channel code[25] was run including reagent and product channels with diatomic rotational quantum number $j_{max} = 16$, and total energies $E_{max} = 1.4$ eV in the basis set. This resulted in 1086 coupled channels for calculations at total angular momentum $J > 3$ for initial $j = 0$. For initial $j = 1$ the maximum number of coupled channels was 795 and 1084 for even and odd parity, respectively. Calculations for up to $J = 26$ were performed in order to obtain well converged integral and differential cross sections.

C. Theoretical simulation of the experimental product kinetic energy distributions

In the experiments by Liu *et al.*,[19] time-of-flight (TOF) spectra of the D-atom product were measured at many laboratory angles (θ_L) at the collision energies $E_c = 86.7$ and 138.8 meV

(2 and 3.2 kcal mol^{-1}, respectively). These TOF spectra were used to derive center-of-mass (CM) product kinetic energy distributions at a given laboratory angle, $P(E'_T;\theta_L)$, by using a standard Jacobian transformation and taking into account the different detection efficiency of the D-atoms at different angles and different velocities.[19] The reported $P(E'_T;\theta_L)$ correspond to the laboratory angles $\theta_L = -60°$ and 117.5° at the low collision energy and $\theta_L = -40°$ and 117.5° at the high collision energy, which in both cases correspond to scattering in the forward and backward directions in the CM frame, respectively.

The simulation of the experimentally derived $P(E'_T;\theta_L)$ with the theoretical fully state-resolved DCSs has been carried out using the experimental rovibrational energies of the OD product and the resolution of the measurements. Due to the high energy resolution of the Rydberg-atom "tagging" technique employed in the experiments, the measured spectra are sensitive to the splitting of the N'-state quadruplets of the OD products due to Λ-doubling and spin-orbit coupling, especially for the peaks associated to the least exothermic states $v' = 3,4$. Thus, in our simulation of the experimental $P(E'_T;\theta_L)$ we have assigned the same cross section to the four states within each N'-manifold (*i.e.*, one fourth of the cross section calculated for the N' state) and we have used the experimental rovibrational energies corresponding to each level. The energy resolution of the experiment has been empirically modeled using the functionality $\Delta E'_T \approx K(E'_T/E'_{max})^{1/4}$, where E'_{max} is the products maximum recoil energy and $K = 150$ cm^{-1} for $E_c = 86.7$ meV and $K = 220$ cm^{-1} for $E_c = 138.8$ meV. The theoretical recoil energy distributions derived from the calculations were scaled to the corresponding experimental $P(E'_T;\theta_L)$ by means of a least-squares procedure (see next section for details).

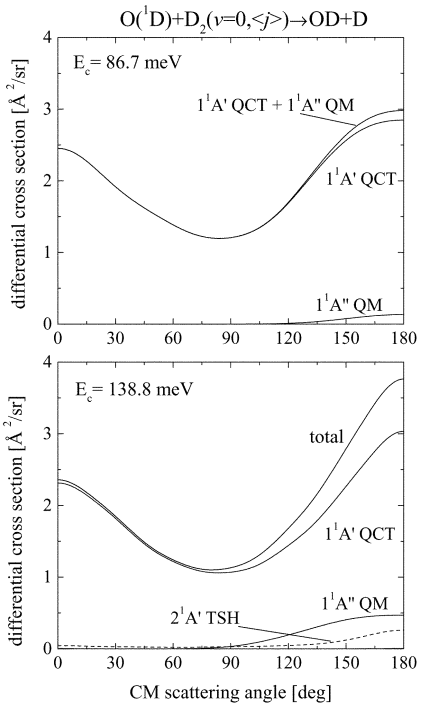

Fig. 1 Total DCS calculated on the DK $1^1A'$ (QCT) and $1^1A''$ (QM) surfaces at 86.7 meV (top panel) and 138.8 meV (bottom panel) collision energies for the $O(^1D) + D_2$ reaction. At both collision energies, a Boltzmann distribution of the rotational quantum number j of the D_2 reagent with 67% in $j = 0$ and 33% in $j = 1$ has been considered. At $E_c = 138.8$ meV, the nonadiabatic calculations on the $2^1A'$ surface by means of a trajectory surface hopping method are shown with a dashed line.

III. Results and discussion

The total reaction cross sections calculated on the three relevant PESs are listed in Table 1 for the two collision energies of interest. At $E_c = 86.7$ meV (2 kcal mol^{-1}), the reactivity is dominated by the ground state $1^1A'$ surface and the contribution from the excited ones is virtually negligible. At $E_c = 138.8$ meV (3.2 kcal mol^{-1}), the cross section for reaction on the $1^1A'$ PES decreases by about 10% with respect to the corresponding one at the low collision energy. At this collision energy, the participation of the excited surfaces in the reaction is still small, but becomes already appreciable; the relative contribution to the total reaction cross section at this energy is about 7% for the $1^1A''$ PES and close to 3% for the $2^1A'$ surface. Note that the increase in rotational excitation of D_2 from $j = 0$ to $j = 1$ enhances the reactivity over the $1^1A''$ PES, but has no effect on the other two surfaces.

Fig. 1 shows the total DCSs calculated on the different surfaces with relative populations of initial $j = 0$ and $j = 1$ of 67% and 33%, respectively. At the lowest collision energy $E_c = 86.7$ meV, the DCS on the $1^1A'$ surface is nearly symmetric with a slight backward preference and the DCS on the $1^1A''$ is backward, but reactive scattering over this latter surface is very small; on the $2^1A'$ PES, reactive scattering is entirely negligible. Given the very small contributions of the excited PESs to the reactivity at this collision energy, the total DCS is essentially determined by the ground state surface and keeps the approximate backward–forward symmetry. At the higher collision energy, $E_c = 138.8$ meV, the slight backward preference observed at the lower energy for scattering over the $1^1A'$ PES increases slightly. In addition, the significant growth in reactive scattering on the $1^1A''$ is also concentrated in the backward hemisphere. Reactive scattering over the $2^1A'$ plays only a minor role and is spread over the whole angular range, but has also a distinct maximum in the backward region. As a result the total DCS becomes asymmetric with a maximum at 180°.

Table 1 QM ($1^1A''$) and QCT ($1^1A'$ and $2^1A'$) integral cross sections (in Å^2) for the $O(^1D) + H_2(v = 0, j = 0,1)$ reaction at $E_c = 86.7$ meV (2 kcal mol^{-1}) and $E_c = 138.8$ meV (3.2 kcal mol^{-1}) collision energies.

Method	$E_c = 86.7$ meV	$E_c = 138.8$ meV
QCT $1^1A'$ $j = 0$	20.97	18.60
QM $1^1A''$ $j = 0$	0.146	1.278
QCT-TSH $2^1A'$ $j = 0$	—	0.58
QCT $1^1A'$ $j = 1$	20.67	18.47
QM $1^1A''$ $j = 1$	0.239	1.626
QCT-TSH $2^1A'$ $j = 1$	—	0.59

The corresponding DCSs resolved into the final vibrational states of the OD product calculated at $E_c = 86.7$ meV are depicted in Fig. 2. The analysis of the results obtained on the ground state $1^1A'$ PES shows that reactive scattering is very symmetric for most v' states and that the slight backward asymmetry in the $1^1A'$ DCS mentioned in the previous paragraph is due to scattering into the lower v' levels, mostly $v' = 0-2$. For any angle, the reactivity corresponding to a given v' state is always larger on the $1^1A'$ surface than on the first excited $1^1A''$ PES. At the higher collision energy $E_c = 138.8$ meV (see top panel of Fig. 3), the DCSs calculated on the $1^1A'$ PES for the lowest v' levels, and especially for $v' = 0-2$, are also slightly asymmetric with a backward preference. In this case, the scattering from the $1^1A''$ and $2^1A'$ surfaces, which is concentrated in the backward region, can compete with that from the ground state surface for some of the v' levels. In particular, for $v' = 5$, which is the most populated vibrational state from the reaction on the excited PESs, the reactive yield from the $1^1A''$ surface is higher than that

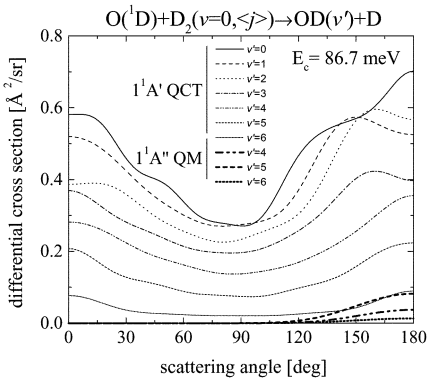

Fig. 2 Vibrationally state-resolved DCS calculated on the DK $1^1A'$ (QCT) and $1^1A''$ (QM) surfaces at 86.7 meV collision energy for the $O(^1D) + D_2$ reaction. A Boltzmann distribution of the initial j of the D_2 reagent with 67% in $j = 0$ and 33% in $j = 1$ has been considered. Notice that the QM calculations on the $1^1A''$ PES are presented by thick lines.

from the $1^1A'$ PES in the 120–170° angular range. For this vibrational state, the reactive scattering from the $2^1A'$ surface is also concentrated in the backward hemisphere as shown in the lower panel of Fig. 3, where the DCS corresponding to the coupled dynamics on the $[1^1A' + 2^1A']$ is shown. A similar behavior (not shown for clarity of display) is obtained for $v' = 6$. For $v' < 5$, the contribution from the $1^1A'$ and $2^1A''$ surfaces is negligible.

The experimental recoil energy distributions reported by Liu *et al.*[19] at $E_c = 86.7$ meV and 138.8 meV have been simulated with the theoretical data of this work (see the "method" section for details on the simulation procedure), and the results of the simulation are shown in Fig. 4. As mentioned above, for the two collision energies studied the reactive scattering was measured at two laboratory angles, one of them corresponding to the forward and the other to the backward CM regions. Since the main aim of the present study is the attempt

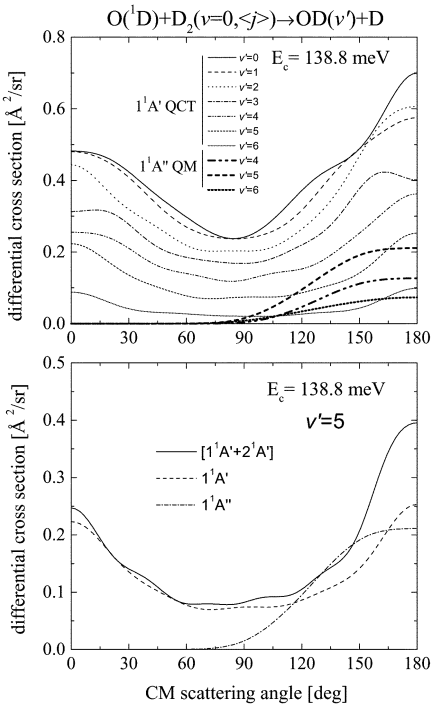

Fig. 3 Top panel: same as in Fig. 2 but for 138.8 meV collision energy. Bottom panel: $v' = 5$ state-resolved DCS calculated adiabatically on the DK $1^1A'$ (QCT) and $1^1A''$ (QM) surfaces at 138.8 meV and nonadiabatically (TSH) on the $[1^1A' + 2^1A'']$ surfaces.

to elucidate theoretically whether a contribution of the excited potential surfaces is apparent in the measurements corresponding to the CM backward angular range, the theoretical results have been scaled by means of a least-squares procedure to the experimental data corresponding to the CM forward region ($\theta_L = -60°$ and $\theta_L = -40°$ for $E_c = 86.7$ and 138.8 meV, respectively), where no reactive scattering from the excited PESs is predicted; the factor thus obtained is used for the comparison with the data at the CM backward angle ($\theta_L = 117.5°$).

At $E_c = 86.7$ meV, the experimental $P(E'_T,\theta_L)$ were reported at the laboratory angles (see the two upper panels of Fig. 4), $\theta_L = -60°$ (forward in the CM frame) and $\theta_L = 117.5°$ (backward in the CM frame). For both angles, the recoil energy distributions are broad, extending up to 2 eV and exhibit a rich structure. The integration of the experimental $P(E'_T,\theta_L)$ over E'_T yields the same value (within 5%) for the two angles, however the theoretical value at $\theta_L = 117.5°$ is higher by about 20% than that at $-60°$. In spite of this difference, there is a reasonably good agreement between the theoretical and experimental recoil energy distributions; the location of the peaks and the broader features are well reproduced in the theoretical simulation, but some discrepancies are observed in the relative intensities. A closer analysis shows that the peak structure observed is caused by the higher rotational states of the low vibrational levels of OD, whose energetic separation increases with growing N' (see below). In general the individual peaks do not correspond to a single rotational level, but rather to a small group of N' levels from different v' states. At the higher end of the distribution, for energies larger than ≈1.5 eV, the peak structure is practically blurred. In this energy range, the available rotational states of OD are closely spaced and are not resolved in the experiment. The experimental $P(E'_T,\theta_L)$ for $\theta_L = 117.5°$ has a maximum at about 0.35 eV. The location of this maximum is well reproduced in the calculations, but its relative intensity is clearly overestimated. At the lower energy range, the theoretical peaks tend to be higher than the experimental ones for the two scattering angles considered. This energetic region corresponds to that of the highest rotational levels accessible and their populations tend to be overestimated by the "binning" procedure for the assignment of final rovibrational levels of the product molecule inherent to the QCT method.

The experimental recoil energy distributions at $E_c = 138.8$ meV were measured for laboratory angles of $\theta_L = -40°$ (forward in the CM frame) and 117.5° (backward in the CM frame) and are displayed in the lower left panel of Fig. 4. The corresponding theoretical simulations are also shown on the lower right panel of the same figure. In this case, noteworthy differences between the two experimental $P(E'_T,\theta_L)$ are obvious at first sight. The amount of reactive scattering at $\theta_L = 117.5°$ is markedly larger than that at $\theta_L = -40°$. The integration in E'_T of the experimental recoil energy distributions shows that the overall reactive yield for the backward angle is larger than that for the forward angle by about 50%. This relative excess of backward scattering is concentrated in the recoil energy range between 0 and 1 eV with a pronounced maximum at about 0.5 eV. For larger E'_T values the two distributions bear a great similarity both in shape and in magnitude. At this collision energy, the experimental resolution in $P(E'_T,\theta_L)$ is worse than at $E_c = 86.7$ meV (see upper panels of Fig. 4) due to the broader velocity distribution of the D_2 beam, which, in order to attain a higher E_c, is expanded from a room temperature source.[19] As indicated above, the theoretical results were scaled to the experimental $P(E'_T,\theta_L)$ corresponding to forward in the CM frame, where the theoretical predictions give only reactive scattering on the $1^1A'$ ground state surface. For this laboratory angle ($\theta_L = -40°$), the simulation of the experimental recoil energy distribution with the theoretical results leads to a global good agreement with some

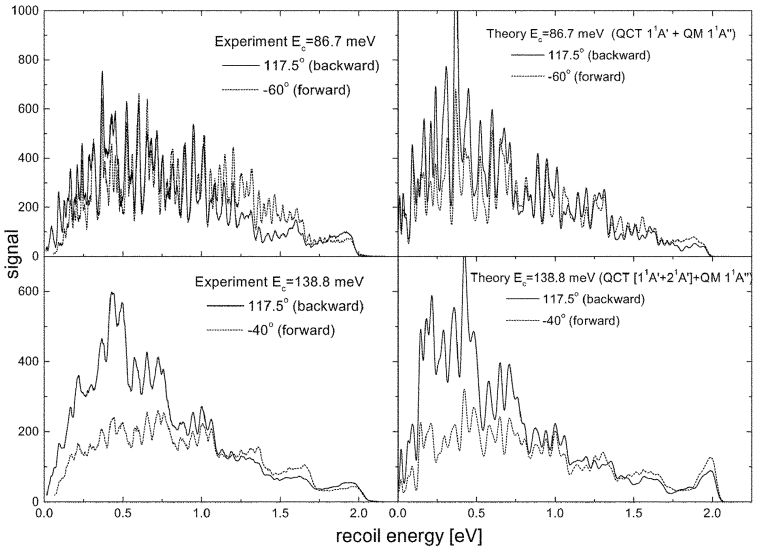

Fig. 4 Experimental (left panels) and theoretical (right panels) product translational energy distributions at the laboratory angles $\theta_L = -60°$ and 117.5° for 86.7 meV collision energy and at $\theta_L = -40°$ and 117.5° for 138.8 meV collision energy. Notice that the laboratory angles $\theta_L = -60°$ at $E_c = 86.7$ meV and $\theta_L = -40°$ at $E_c = 138.8$ meV correspond to forward scattering in the CM frame, whereas $\theta_L = 117.5°$ at both collision energies corresponds to CM backward scattering. At each collision energy, the theoretical $P(E'_T;\theta_L)$corresponding to CM forward scattering has been scaled to the experimental one by means of a least-squares procedure. The scaling factor thus obtained has been used to scale the corresponding data for CM backward scattering.

discrepancies. Among these discrepancies it is worth noticing the relatively high theoretical peak at the highest recoil energies ($E'_T \approx 2$ eV), which has no experimental counterpart. As in the previous case, the theoretical simulation demonstrates that the experimental peaks correspond in general to small groups of high rotational levels of the lowest vibrational states of OD.

In the CM backward region pertinent to the experimental measurement at $E_c = 138.8$ meV, the calculations yield appreciable reactive scattering also on the $1^1A''$ surface (see Fig. 1). At $\theta_L = 117.5°$, the global theoretical reactive yield obtained by integration of the corresponding $P(E'_T,\theta_L)$, is larger by 57% than that at $\theta_L = -40°$, in good agreement with the experimental observations. Again in this case, the overall shape and magnitude of the measured recoil energy distribution is well reproduced in the simulation, but some discrepancies appear in the relative intensities, notably in the lower energy region (below 0.5 eV). As already mentioned, this region corresponds to the highest rotational levels accessible that tend to be overpopulated by the "binning" procedure used to assign the internal states in the QCT method. This overpopulation of the highest N' levels could lead to a distortion of the theoretical recoil energy distribution.

In order to gain more insight into the details of the different mechanisms responsible for the backward reactive scattering at $E_c = 138.8$ meV, the theoretical $P(E'_T,\theta_L)$ for the coupled $[1^1A' + 2^1A']$ PESs and the $1^1A''$ PES at the laboratory angle $\theta_L = 117.5°$ are separated in Fig. 5. The contribution of the $2^1A'$ surface to the $P(E'_T,\theta_L)$ at $\theta_L = 117.5°$ is very small and the recoil energy distribution corresponding to the sum of the reactive scattering over $1^1A'$ and $2^1A'$ hardly changes with respect to that over $1^1A'$ alone (not shown). Fig. 6 shows the theoretical recoil energy distribution calculated on the $1^1A'$ surface resolved into the individual vibrational levels of the OD product. The latter figure shows that the reaction on the largely attractive $1^1A'$ surface leads to molecules with a broad distribution of vibrational and rotational states spanning the whole range of recoil energies available; it is now clear that the peak structure appearing in all the $P(E'_T,\theta_L)$ for recoil energies lower than ≈1 eV is largely caused by OD molecules in the highest rotational levels of the lower v' states, as indicated above. In general, several N' values, corresponding to different vibrational states are grouped under each of the peaks of the total $P(E'_T,\theta_L)$. The broad and almost structureless "steps" observed in the recoil energy distributions for E'_T larger than 1 eV correspond to the lowest rotational levels of $v' = 0,1$ and 2, which are too closely spaced to be resolved in the experiment. For all the cases considered in this article, the part of the experimental $P(E'_T,\theta_L)$ beyond $E'_T = 0.85 - 1.10$ eV has also this origin. At $E_c = 138.8$ meV, the theoretically predicted reactive scattering (obtained by integrating $P(E'_T,\theta_L)$ over E'_T) at $\theta_L = 117.5°$ just on the ground $1^1A'$ surface is a factor of 1.37 larger than that obtained on the same PES for the forward angle. This accounts for a large part of the increase in backward scattering observed in the experiment.

The $1^1A''$ PES contributes approximately by 13% to the predicted total reactive scattering. The reaction on this surface, characterized by an abstraction mechanism, produces OD molecules in high vibrational and comparatively low rotational

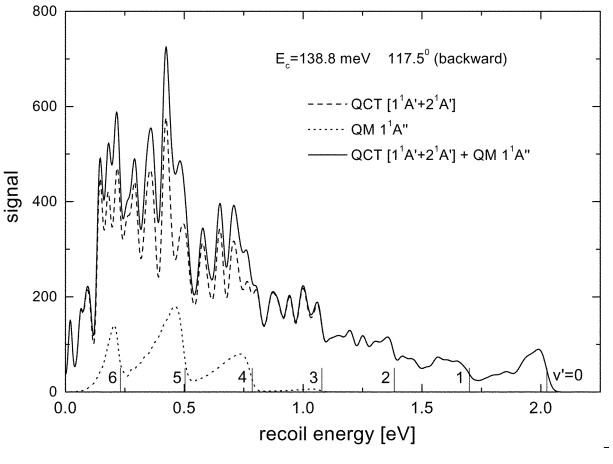

Fig. 5 Total product translational energy distribution at $\theta_L = 117.5°$ for $E_c = 138.8$ meV (solid line) and the contributions from the coupled dynamics on the $1^1A' + 2^2A'$ surfaces (dashed line) and from the excited $1^1A''$ surface (dotted line). The vertical lines indicate the opening of the different v' channels of the OD product.

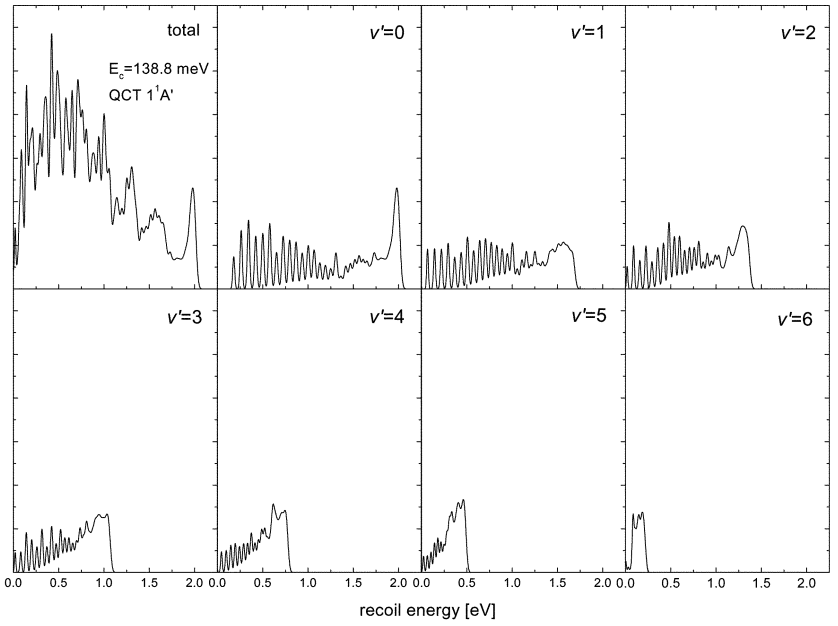

Fig. 6 QCT total and vibrationally state-resolved product translational energy distribution for $E_c = 138.8$ meV at $\theta_L = 117.5°$ (CM backward scattering) calculated on the ground state $1^1A'$ surface.

states leading to broad features in the low E'_T range of the theoretical $P(E'_T,\theta_L)$ distribution, which can be identified with scattering into the $v' = 4$, 5 and 6 levels of OD, but without resolution, even partial, into the final rotational states (see Fig. 5). These broad peaks modulate and smear slightly the finer peak structure obtained on the ground state PES and enhance the global intensity of $P(E'_T,\theta_L)$ for E'_T lower than ≈1 eV.

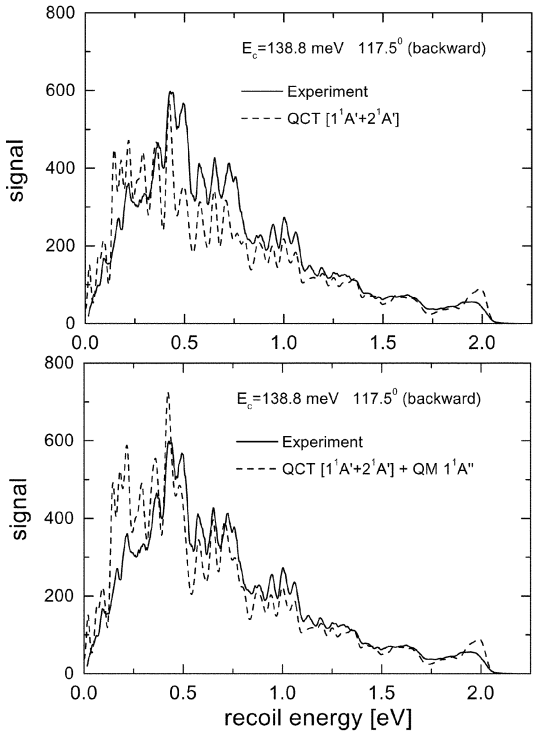

Fig. 7 Experimental and theoretical product translational energy distribution at $\theta_L = 117.5°$ for $E_c = 138.8$ meV. Top panel: the theoretical simulation corresponds to QCT calculations on the coupled $1^1A' + 2^1A'$ surfaces. Bottom panel: the theoretical simulation corresponds to the sum of the QCT calculations on the coupled $1^1A' + 2^1A'$ surfaces and the QM calculations on the excited $1^1A''$ surface.

In Fig. 7 the theoretical recoil energy distributions for $E_c = 138.8$ meV at $\theta_L = 117.5°$ with and without the contribution of the $1^1A''$ surface are compared to the corresponding experimental one. It should be recalled once more that the comparison is performed in an absolute scale with a single scaling factor derived from a fit of the experimental forward scattering data at the same collision energy. The upper panel of this figure shows that much of the experimental $P(E'_T,\theta_L)$ can be accounted for without invoking the participation of the $1^1A''$ PES. The calculated amount of reactive scattering in the ≈0.5 and 1 eV E'_T range is lower than that obtained in the experiment. On the other hand, for recoil energies lower than ≈0.3 eV, the theoretical values are higher than the measured ones. When the reactive scattering over the $1^1A''$ surface is also included in the simulation, the agreement between theory and experiment is definitely better between 0.5 and 1 eV, but the disagreement below 0.3 eV is also increased.

IV. Conclusions

Adiabatic quasiclassical trajectory and quantum mechanical scattering calculations have been carried out on the ground $1^1A'$ and first excited $1^1A''$ potential energy surfaces developed by Dobbyn and Knowles for the $O(^1D) + D_2(v = 0, j = 0,1)$ reaction with the aim of simulating high resolution crossed molecular beam experiments recently reported by Liu *et al.*[19] employing the D-atom Rydberg "tagging" technique. Non-adiabatic contributions from the excited $2^1A'$ surface to the reaction have been considered by means of a trajectory surface hopping methodology.

The experimental data in the form of center-of-mass product translational energy distributions at selected laboratory scattering angles, $P(E'_T;\theta_L)$, obtained at two collision energies (86.7 and 138.8 meV) have been simulated using the theoretical fully state-resolved differential cross sections.

The experimental results indicate an increase in the center-of-mass backward scattering with growing collision energy, which was attributed to the contribution of the excited $1^1A''$ potential surface.[19] Although the present theoretical results show that at the higher collision energy there is a considerable contribution of the excited $1^1A''$ surface, it is demonstrated

that a substantial part of the increase of reactive yield into the backward region is due to the ground state $1^1A'$ PES. In any case, the best agreement with experiment is found when both the $1^1A'$ and $1^1A''$ surfaces are considered. The contribution of non-adiabatic transitions from the excited $2^1A'$ surface is very minor.

The discrepancies found between theory and experiment may be due to the possibly hotter rotational distributions of the OD products obtained in the QCT calculation in comparison with the experimental results. These hotter rotational distributions obtained theoretically are due to the "binning" procedure employed to assign final rovibrational states of the OD products. This limitation of the QCT method might be responsible for the distortion of the $P(E'_T;\theta_L)$ found in the low E'_T range.

Acknowledgements

We thank Prof. Xueming Yang who kindly sent us the experimental data of Fig. 4 and 7. JFC acknowledges financial support by the Spanish Ministry of Science and Technology through the program "Ramón y Cajal". BMH acknowledges financial support from the "Plan Andaluz de Investigación" (group FQM-205). This work has been financed by the DGES of Spain under contracts PB98-0762-C03 and REN-2000-1557-CL1, and by the EU Research Training Network "Reaction Dynamics" HPRN-CT-1999-00007. The facilities provided by the Centro de Supercomputación Complutense (SG Origin 2000) are gratefully acknowledged.

References

1 P. Casavecchia, *Rep. Prog. Phys.*, 2000, **63**, 335.
2 K. Liu, *Annu. Rev. Phys. Chem.*, 2001, **52**, 139.
3 G. Durand and X. Chapuisat, *Chem. Phys.*, 1985, **96**, 381.
4 T.-S. Ho, T. Hollebeek, H. Rabitz, L. B. Harding and G. C. Schatz, *J. Chem. Phys.*, 1996, **105**, 10472.
5 G. C. Schatz, A. Papaioannou, L. A. Pederson, L. B. Harding, T. Hollebeek, T. S. Ho and H. Rabitz, *J. Chem. Phys.*, 1997, **107**, 2340.
6 (*a*) A. J. Dobbyn and P. J. Knowles, *Mol. Phys.*, 1997, **91**, 1107; (*b*) A. J. Dobbyn and P. J. Knowles, *Faraday Discuss.*, 1998, **110**, 247.
7 D.-C. Che and K. Liu, *J. Chem. Phys.*, 1995, **103**, 5164.
8 Y.-T. Hsu and K. Liu, *J. Chem. Phys.*, 1997, **107**, 1664.
9 Y.-T. Hsu, J.-H. Wang and K. Liu, *J. Chem. Phys.*, 1997, **107**, 2351.
10 A. J. Alexander, F. J. Aoiz, L. Bañares, M. Brouard, J. Short and J. P. Simons, *J. Phys. Chem. A.*, 1997, **101**, 7544.
11 A. J. Alexander, D. A. Blunt, M. Brouard, J. P. Simons, F. J. Aoiz, L. Bañares, Y. Fujimura and M. Tsubouchi, *Faraday Discuss.*, 1997, **108**, 375.
12 M. Alagia, N. Balucani, L. Cartechini, P. Casavecchia, E. H. van Kleef, G. G. Volpi, P. J. Kuntz and J. J. Sloan, *J. Chem. Phys.*, 1998, **108**, 6698.
13 M. Ahmed, D. S. Peterka and A. G. Suits, *Chem. Phys. Lett.*, 1999, **301**, 372.
14 Y.-T. Hsu, K. Liu, L. A. Pederson and G. C. Schatz, *J. Chem. Phys.*, 1999, **111**, 7921.
15 Y.-T. Hsu, K. Liu, L. A. Pederson and G. C. Schatz, *J. Chem. Phys.*, 1999, **111**, 7931.
16 F. J. Aoiz, L. Bañares, J. Castillo, M. Brouard, W. Denzer, C. Vallance, P. Honvault, J. M. Launay, A. Dobbyn and P. Knowles, *Phys. Rev. Lett.*, 2001, **86**, 1729.
17 X. Liu, J. J. Lin, S. Harich and X. Yang, *J. Chem. Phys.*, 2000, **113**, 1325.
18 X. Liu, J. J. Lin, S. Harich, G. G. Schatz and X. Yang, *Science*, 2000, **289**, 1536.
19 X. Liu, J. J. Lin, S. Harich and X. Yang, *Phys. Rev. Lett.*, 2001, **86**, 408.
20 F. J. Aoiz, L. Bañares, J. F. Castillo, V. J. Herrero, B. Martínez-Haya, P. Honvault, J.-M. Launay, X. Liu, J. J. Lin, S. A. Harich, C. C. Wang and X. Yang, *J. Chem. Phys.*, 2002, **116**, 10692.
21 F. J. Aoiz, L. Bañares and V. J. Herrero, *J. Chem. Soc. Faraday Trans.*, 1998, **94**, 2483.
22 F. J. Aoiz, L. Bañares, M. Brouard, J. F. Castilo and V. J. Herrero, *J. Chem. Phys.*, 2000, **113**, 5339.
23 F. J. Aoiz, L. Bañares, J. F. Castillo, B. Martínez-Haya and M. P. Miranda, *J. Chem. Phys.*, 2001, **114**, 8328.
24 S. K. Gray, C. Petrongolo, K. Drukker and G. Schatz, *J. Phys. Chem. A.*, 1999, **103**, 9488.
25 D. Skouteris, J. F. Castillo and D. E. Manolopoulos, *Comput. Phys. Commun.*, 2000, **133**, 128.